LAWRENCE
LIVERMORE
NATIONAL
LABORATORY

UCRL-CONF-200512

Development and testing of the improved focusing quadrupole for heavy ion fusion accelerators

N. N. Martovetsky, R. R. Manahan, R. B. Meinke, L. Chiesa, A. F. Lietzke, G. L. Sabbi, P. A. Seidl

October 23, 2003

18th International Conference on Magnet Technology
Morioka, Japan
October 20, 2003 through October 24, 2003

UCRL-CONF-200512

Development and Testing of the Improved Focusing Quadrupole for Heavy Ion Fusion Accelerators

Nicolai N. Martovetsky, Robert R. Manahan, Rainer B. Meinke, Luisa Chiesa, Alan F. Lietzke, GianLuca Sabbi, Peter A. Seidl

***Abstract*— An improved version of the focusing magnet for a Heavy Ion Fusion (HIF) accelerator was designed, built and tested in 2002-2003. This quadrupole has higher focusing power and lower error field than the previous version of the focusing quadrupoles successfully built and tested in 2001. We discuss the features of the new design, selected fabrication issues and test results.**

***Index Terms*— Superconducting accelerator magnets, Superconducting device testing, magnetic variables measurement.**

I. Introduction

THE U.S. community has been exploring induction-based accelerators, with the baseline approach a linear-induction accelerator. The driver has multiple beams (100-200) in transverse quadrupole arrays that threads common induction cores for acceleration. Possible limitations on the transportable current are beam centroid oscillations due to alignment imperfections, envelope mismatch, and the deterioration of focusing field quality at large radii due to higher multipole components in the body of the lens and its ends. Compact designs that minimize the structure between adjacent beams (coils, supports) are desirable to minimize the focusing array size and in turn the amount of induction core material needed for economical acceleration. With these considerations in mind, we have pursued the design of quadrupoles suitable for one-beam experiments [1] aimed at exploring the limitations on the transportable current and the ratio of the maximum beam-envelope radius to the beam pipe radius while preserving the focusability of the beam(s) on the fusion target.

A new concept of economical quads was developed, built and tested in 2000-2001 [2]. These magnets used racetrack coils, which provided very good performance with little or no training and no degradation. For a single beam focusing magnet, the racetrack design theoretically is somewhat less efficient than the traditional "cosine 2θ" design from the standpoint of the amount of conductor for a fixed gradient. On the other hand, the racetrack is easier and less expensive to fabricate and small or no degradation and training reduces or eliminates advantages of the traditional design in practice. In the future multi beam accelerators for fusion power plants the magnets will be used in the form of arrays. The performance difference between the racetrack and the "modified cosine 2θ" concepts for arrays becomes even less significant due to flux sharing, while economic advantages of the racetrack make it a very attractive option. Simple racetrack magnets developed for the single beam accelerators would be applicable to future multi-aperture arrays, since basic elements of the coils and many fabrication steps will be similar.

The quadrupole presented in this paper was developed in a collaborative effort among LLNL, AML and LBNL with some support from MIT PFSC. LLNL developed the concept, performed thermal, structural, electromagnetic analysis, designed the quadrupole, procured the parts, designed tooling, built some of the tools for fabrication of the magnet, transferred the technology to the industrial partner, AML, and assisted in magnet fabrication. LLNL designed the experimental set up, provided some parts, participated in the test at LBNL and performed some post test analysis.

The AML, Inc. built the rest of the tools, fabricated the magnet and established all manufacturing steps. LBNL supplied the superconducting cable, modified facility to accommodate the test, carried out the tests and performed post test analysis.

The MIT PFSC verified some analyses, participated in key discussions and provided their expertise in selection of

Manuscript received October 21, 2003. This Work supported by the US Department of Energy under contract to the Lawrence Livermore National Laboratory (contract No. W-7405-Eng-48) and to the Lawrence Berkeley National Laboratory (DE-AC03-76SF00098).

N.N.M. and R.R.M. are with Lawrence Livermore National Laboratory, Livermore, CA 94550, USA, (telephone (925) 422 4269, e-mail: martovetsky1@llnl.gov)

R.B.M. is with Advanced Magnetic Laboratory, 2730 Kirby Ave., Palm Bay, Fl, 32905, USA (telephone (321) 728 7543, e-mail: rmeinke@magnetlab.com)

L.C., A.F.L., GL. S and P.A.S are with Lawrence Berkeley National Laboratory, Berkeley, CA, 94720, USA, (telephone (510) 486 4572, e-mail: aflietzke@lbl.gov) .L.C. is currently with MIT Plasma Science and Fusion Center, Cambridge, MA, 02139 USA, e-mail: lchiesa@mit.edu

several options.

II. Quadrupole Design

An improved concept was developed based on our earlier quadrupole work [2]. The quadrupole consists of four quadrants, surrounded by an iron yoke with the OD of 260 mm. The coil holders are 136 mm long, and the square aperture is 72.5 mm.

Fig. 1 shows one quadrant of the quadrupole coils for the previous design (left) and for the improved design (right). We modified the ends of the racetrack to make it as rectangular as possible, which was limited by the tightest practical conductor bend radius.

This modification was partially inspired by work [3], which showed that the rectangular turns winding may significantly suppress the error field generated by the coil ends. The improved design was intended to improve performance of the quad for different reasons. First, in the old design the semicircular ends created a significant error field. To compensate the integrated field error, we had to reduce number of turns in the straight runs, which decreased the gradient. In the new design, since we do not have to compensate for the field error, we have more turns in the straight leg and therefore higher gradient.

Second, the effective length of the quad increased due to longer straight leg of the racetrack, which increases the focusing power. Third, in the old design, the peak field in the coil occurred at the inner radius in the ends. This location is not directly relevant to the maximum gradient; it is more efficient when the peak field is located on the straight leg. With the new geometry, the peak field moves to the straight leg, and thus the superconductor use is more efficient than in the old design.

Each one of the abovementioned mechanisms gives 4-7% improvement in focusing power, but combined together they give a sizable effect. Fig. 3 shows comparison in performance between the old and improved versions of the quadrupole. In addition to increased gradient, the new design also gives lower local error fields, while the previous design required

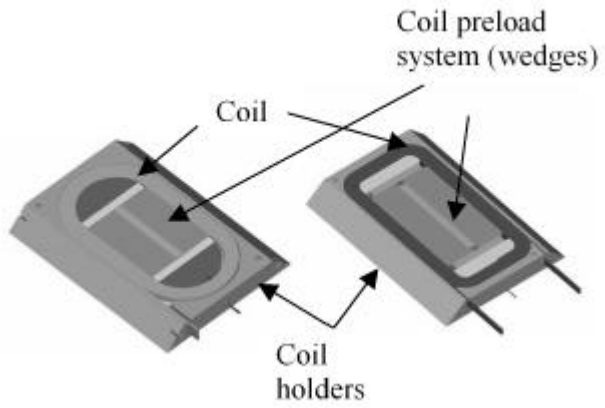

Fig. 1. Previous design (left) and improved design (right) of the racetrack coils for focusing quadrupole. Four units make a quadrupole.

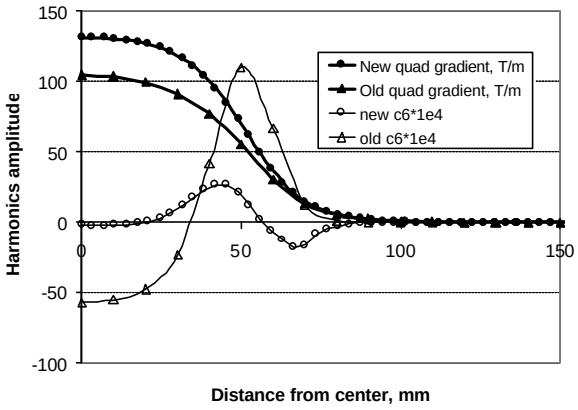

Fig.2. Comparison between previous and the new design, gradient and error field harmonic c6 at 500 A/mm2 winding pack current density.

body-end compensation to optimize the integrated field quality. The definition of error field is given below in this paper in section IV.

Cost trade off studies and structural analysis indicated that a high strength aluminum would be more economical option for the coil holder and after cooldown would provide higher prestress on the winding pack than a stainless steel coil holder used in the previous prototype. Therefore we selected a high strength aluminum alloy 7075-T6.

III. Fabrication Issues

The fabrication steps of this prototype are identical to the previous effort [2], but the modified design required some adjustments. The price for the improved performance of the new design is more difficult fabrication and more difficult support of the ends. The mechanical stability of the semi round ends in the old design is much better than straight runs in the new design, which now requires strong preload of the turns for low training and degradation of the magnet. One of the goals of the project was to find out if improved version is feasible with low training and degradation, since current densities in the winding pack reach extremely high values up

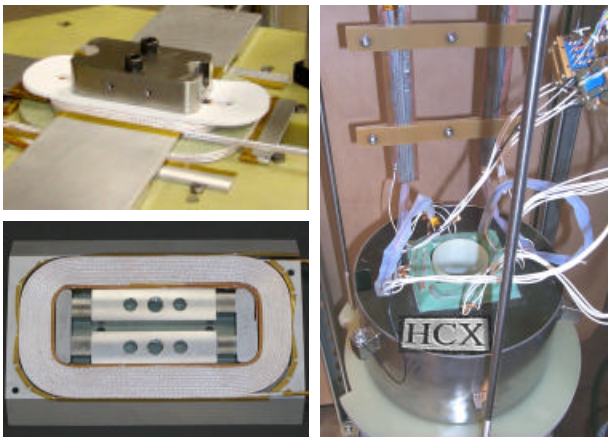

Fig. 3: Quadrupole coil fabrication (left). Completed magnet undergoing test preparations (right).

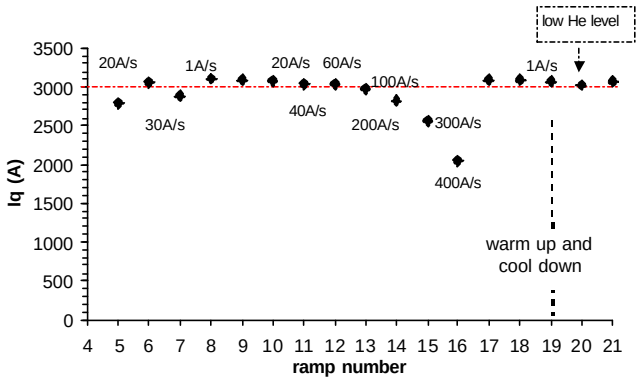

Fig. 4. Quench history, showing ramp rates of the runs. Dash-dot line indicates maximum achievable expectations.

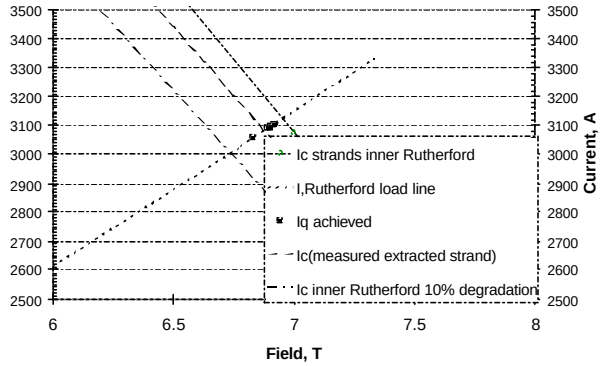

Fig. 6. Cable performance in the quadrupole versus original strand and strand extracted from the cable performance

to 500-550 A/mm^2.

Despite excellent results reached with the APC conductor in the previous project with the old design, we used the Rutherford cable in the new magnet for several reasons; the most important was that the peak field grew to 7 T, where the APC conductors have inferior properties to that of conventional multifilament superconductors. We used the strands for the SSC dipole inner layer with Cu:NbTi ratio of 1.3 redrawn down to 0.648 mm. The cable had 13 strands with final dimension of 4.05x1.17 mm, the same size as the Rutherford cable used in our first prototype effort [2]. Due to higher NbTi content (the previously used cable was made out of the outer SSC strand with Cu:NbTi ratio of 1.8) and significant amount of cold work in the strands, the new cable was significantly stiffer. This created some problems for fabrication, especially in the corner where the tight bending radius was required. We managed to wind the racetracks with 6 mm bend radius, but the cable started losing its shape at the bends. It grew in width and the strands rotated exposing sharp corners to the insulation, which created a risk of shorts. To give the winding pack good integrity and strength, we used the S-glass insulation, which was not very robust before impregnation. Handling the stiff cable with such sharp radius of curvature turned out to be difficult but manageable. However, for mass production it may be necessary to introduce some improvements, like cable annealing and/or increasing the bend radius somewhat or using a monolith conductor, which changes its form much less.

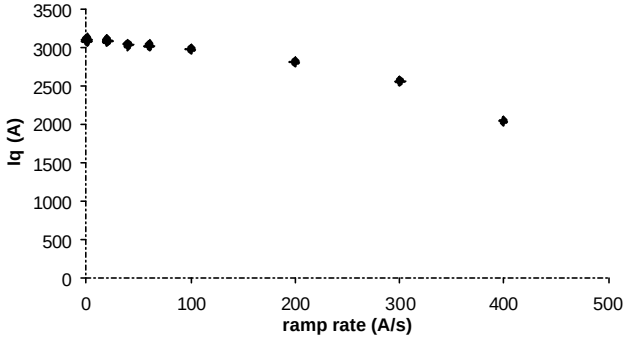

Fig. 5. Ramp rate sensitivity of the quadrupole

Some adjustments with respect to the design geometry were necessary during magnet fabrication, in particular to accommodate a larger than expected cable size, and higher deflections of the aluminum coil holders. Such modifications contributed to deviations from the design field quality and the generation of non-allowed harmonics (per section IV). These effects will be taken into account in future design iterations. Fig. 3 shows some snap shots in quadrupole fabrication.

IV. Test Results

The quadrupole was tested in a vertical cryostat filled with liquid helium. In order to measure field quality in the quadrupole, we built an anti-cryostat to house a pick up rotating coil.

1) Training, degradation, ramp rate sensitivity

The quadrupole had very low training; the history is shown in Fig. 4. After several trips at low currents (due to power supply noise), the first meaningful charge resulted in a quench current of about 93% of the sum of the strands critical currents at the peak field. The second charge to quench reached close to the short sample current in the peak field of 7 T. Ramp rates below 100 A/s did not affect the quench current, as shown in Fig.5. This means there are low losses in the magnet and a uniform current distribution. This behavior is similar to the previous prototype with the Rutherford cable [2].

Warm up to room temperature did not affect quench current on the following charges, which indicates good mechanical stability of the quadrupole windings. Fig. 6 compares the quadrupole performance data with the critical current of the strand extracted from the cable and with expected bounds of the cable critical current for two cases: 10% degradation due to cabling and compacting and without degradation. It shows almost full utilization of the superconducting properties of the strand in the magnet. Measurements of the joint resistances showed that they were

below 2 nOhms, which is acceptable.

2) Field quality measurements system

Magnetic measurements were performed using the LBNL vertical drive, rotating coil system. We used a 44.5 mm diameter, 82 cm long probe, fabricated for the US-LHC quadrupole R&D program [4], provided by FNAL. Special bearings support and align the probe at the center of an anti-cryostat inserted in the magnet bore to allow room temperature access. The probe assembly is connected to the VMA, a precision mechanism allowing vertical motion and rotation at constant speed (0.7 Hz for this test). The probe has 5 windings on a machined ceramic probe form: a main tangential winding for measurement of all field harmonics, as well as dedicated dipole and quadrupole windings measuring the lowest order components of the field. The dual quadrupole correction coils were wired to provide a high-resolution harmonic signal by suppressing the quadrupole component.

The dipole windings were not used for this test. Both the tangential and bucked signals were amplified with integrating amplifiers, digitized at 1 kHz with 24-bit HP3458A DMV's, and Fourier analyzed relative to the fundamental. The resulting harmonics were corrected for the appropriate amplifier gain and coil harmonic sensitivities, and normalized to a radius of 22 mm to compare them with the model calculations.

3) Field representation and analysis

The field is represented in terms of harmonic coefficients defined by the power series expansion:

$$B_y + iB_x = B_2 10^{-4} \sum_{n=1}^{\infty} \bar{c}_n \left(\frac{x+iy}{r_0} \right)^{n-1}$$

where B_x and B_y are the transverse field components, B_2 is the quadrupole field, and $\bar{c}_n = b_n + i\,a_n$ are the multipole coefficients, expressed in 10^{-4} "units" of the quadrupole component. The magnet is oriented such that the magnetic midplanes of the quadrupole field lie along the x and y-axes.

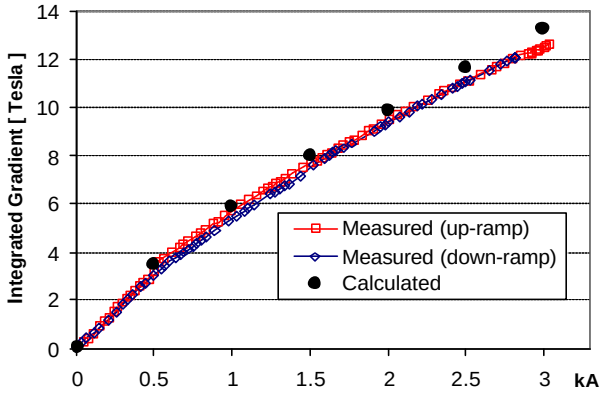

Fig. 7: Integrated gradient as function of current

TABLE I
INTEGRATED HARMONICS

Current (A)	Temp (K)	Data type	Gradient B_2/r_0 (T)	12-pole $\|c_6\|$ (units)	20-pole $\|c_{10}\|$ (units)
9.5	300	Meas. (*)	0.0674	109	15.5
9.5	-	Calc.	0.0726	121	19.1
2500	4.2	Meas.	11.03	5.8	8.5
2500	-	Calc.	11.63	8.1	8.7

(*) Averages for ± 9.5 A current and clock/counterclockwise probe rotation

The z-axis is directed from the return end towards the lead end. Both measurements and calculations are longitudinally integrated over the length of the measurement coil. The magnet powering convention is such to provide a positive value of the quadrupole field component B_2. The reference radius r_0 is 22 mm.

The test plan included both warm and cold magnetic measurements. Warm measurements at low current (9.5 A) were performed to check the probe and data acquisition setup, and to determine the longitudinal reference. At low current, the unsaturated iron inserts and the yoke provide the dominant contribution in shaping the field. Comparisons between warm measurements and calculations for the same current are shown in Table I.

Cold magnetic measurements consisted of current cycles at different ramp rates and longitudinal scans at constant current. The integrated harmonics at the nominal operating current of 2.5 kA are shown in Table I. The 5% discrepancy between measured gradient and design calculations is presently attributed to the tangential integrator response. A calibration effort is underway. The dodecapole shows a 2.3 unit shift, and the 20-pole has a 0.2 unit shift, which can be attributed to deviations from the design geometry, in particular due to larger than expected cable thickness. The transfer function and saturation harmonics are shown in Fig. 7 and Fig. 8. The low-current cold measurements are in better agreement with calculations than those taken at room temperature (Table I). Some discrepancy between calculations and measurements is observed for the

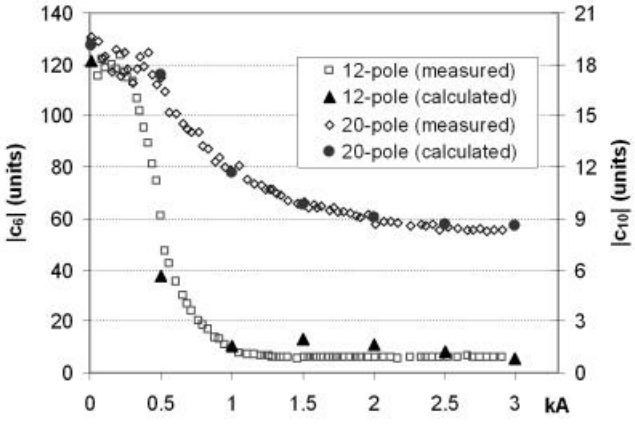

Fig. 8: Integrated harmonics as function of current

TABLE II
NON-ALLOWED HARMONICS VS RANDOM ERRORS (1 SIGMA)

Order n	Measured $\|c_n\|$ (units)	Random-Block $\|c_n\|$ (units)	Random-Quadr. $\|c_n\|$ (units)
3	5.3	2.7	6.5
4	2.5	1.8	1.8
5	7.0	0.8	0.3
7	0.6	0.2	0.5
8	1.0	0.1	0.3
9	2.8	0.05	0.1

dodecapole in the intermediate current range, requiring further analysis.

A dipole component of the order of 3% of the quadrupole field at the reference radius was observed. It corresponds to a misalignment between the probe axis and the magnetic axis of about 0.7 mm.

Non-allowed harmonics caused by departures from the quadrupole symmetry were also observed. These harmonics can be correlated to random field errors due to manufacturing tolerances. In order to estimate the random field errors, two Monte Carlo simulations were performed. In the first case, each conductor block (half-coil) in the magnet cross-section is randomly displaced with respect to its design position, assuming a flat distribution along each axis with a ±100 μm range. In the second case, each quadrant (a subassembly composed of one inner and one outer coil) is displaced by the same amount. For each case, five hundred cross-sections were generated using a computer code ROXIE [5], and the average and rms values of their harmonics were calculated. Table II shows a comparison between the measured non-allowed harmonics and one standard deviation of the Monte Carlo simulations. The measured harmonics for n=3, n=4, n=7 are consistent with the random error estimates. The n=8 component corresponds to about 3 sigma, while the n=5 and n=9 components are too large to be explained based on random displacements. Further analysis is required to understand the cause of these two harmonics.

V. NEXT STEPS

The main goals for the next iteration of prototype fabrication and testing are improving the magnet field quality and further reducing its cost. The coil design will be adjusted to reduce the systematic field errors. A decrease of number of parts and fabrication steps will be pursued. The minimum bending radius may be increased to facilitate coil winding and the use of kapton insulation without impregnation is being considered.

We are also exploring the application of this quadrupole design to multiple beam arrays, where the issues of flux sharing between quadrupole channels, field quality and field termination at the periphery of the array are special concerns for the fusion application. The design and fabrication of a prototype multiple beam array (4 or 9 beam) will be an essential step to address these issues.

VI. CONCLUSIONS

We demonstrated that the developed technology of the prestressed and impregnated racetracks in the coil holders practically eliminated training and degradation in the superconducting coils with very high current densities in the winding pack. Thermal cycles did not affect the magnet performance. The quadrupole showed low sensitivity to the ramp rate. Resistance of the joints was below 2 nOhm. These parameters give a very good basis for development of the focusing arrays for future accelerators.

We showed that our magnets provide the field quality close to the expected values. Future analysis of the test results will give exact modifications in the design to obtain better field quality.

ACKNOWLEDGEMENT

We are grateful to Grant Logan and Wayne Meier for supporting the magnet development effort for Heavy Ion Fusion, the personnel of AML, Inc. for their creative workmanship, Joe Minervini and Joel Schultz from PSFC MIT and A. Zlobin from FNAL for useful discussions and Dan Dietderich from LBNL for strand Ic measurements. We also wish to thank Mike Lamm, Clark Reid, Phil Schlabach and Cosmore Sylverster from FNAL for providing a large-diameter rotating probe for magnetic measurements. Ray Hafalia and Roy Hannaford (LBNL) led the effort to design and fabricate a new cryostat header and anticryostat to house the FNAL probe. The support of the magnet testing team at LBNL, in particular Paul Bish, Bill Lau, Mark Nyman and Sara Mattafirri, was also essential for the success of this test.

REFERENCES

[1] J. J. Barnard, L. E. Ahle, F. M. Bieniosek, C. M. Celata, R. C. Davidson, D. P. Grote, E. Henestroza, A. Friedman, J. W. Kwan, B. G. Logan, E. P. Lee, S. M. Lund, W. R. Meier and H. Qin, "Integrated Experiments for Heavy Ion Fusion,"? Laser and Particle Beams **21**, in press (2003).

[2] N. Martovetsky, R. Manahan, A. Lietzke, "Development of Superconducting Focusing Quadrupoles for Heavy Ion Drivers", IEEE Transactions on Applied Superconductivity v.12, N 1 March 2002, p. 157-160.

[3] L. Myatt, Quadrupole Prototype Design Review (Field and Structural Analysis). HCX memo 0012-04, Dec. 2000, unpublished.

[4] P. Schlabach et al., "Field Quality in Fermilab-built Models of Quadrupole Magnets for the LHC Interaction Regions", IEEE Trans. Appl. Superconduct., vol. 11, no. 1, March 2001, pp. 1566.

[5] S. Russenschuck (editor) "ROXIE: Routine for the Optimization of magnet X-sections, Inverse field calculation and coil End design", First International Roxie Users Meeting and Workshop, CERN 99-01, 1999.

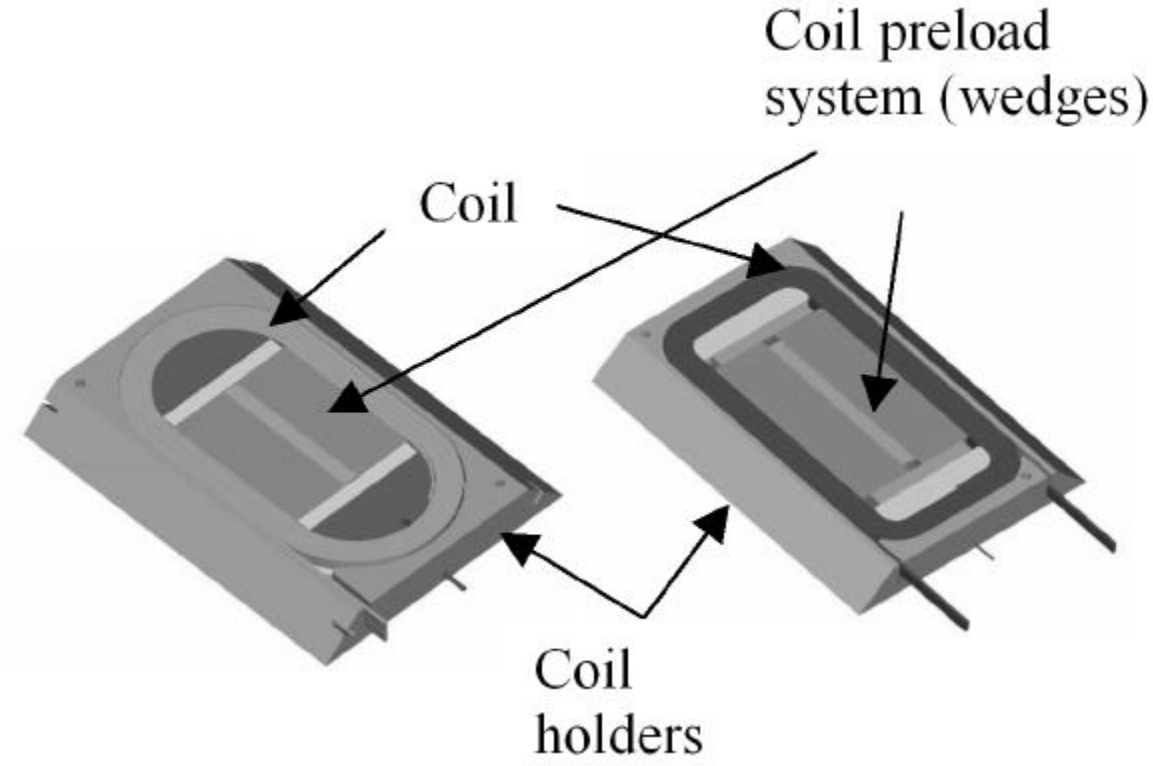
Coil preload
system (wedges)
Coil
Coil
holders

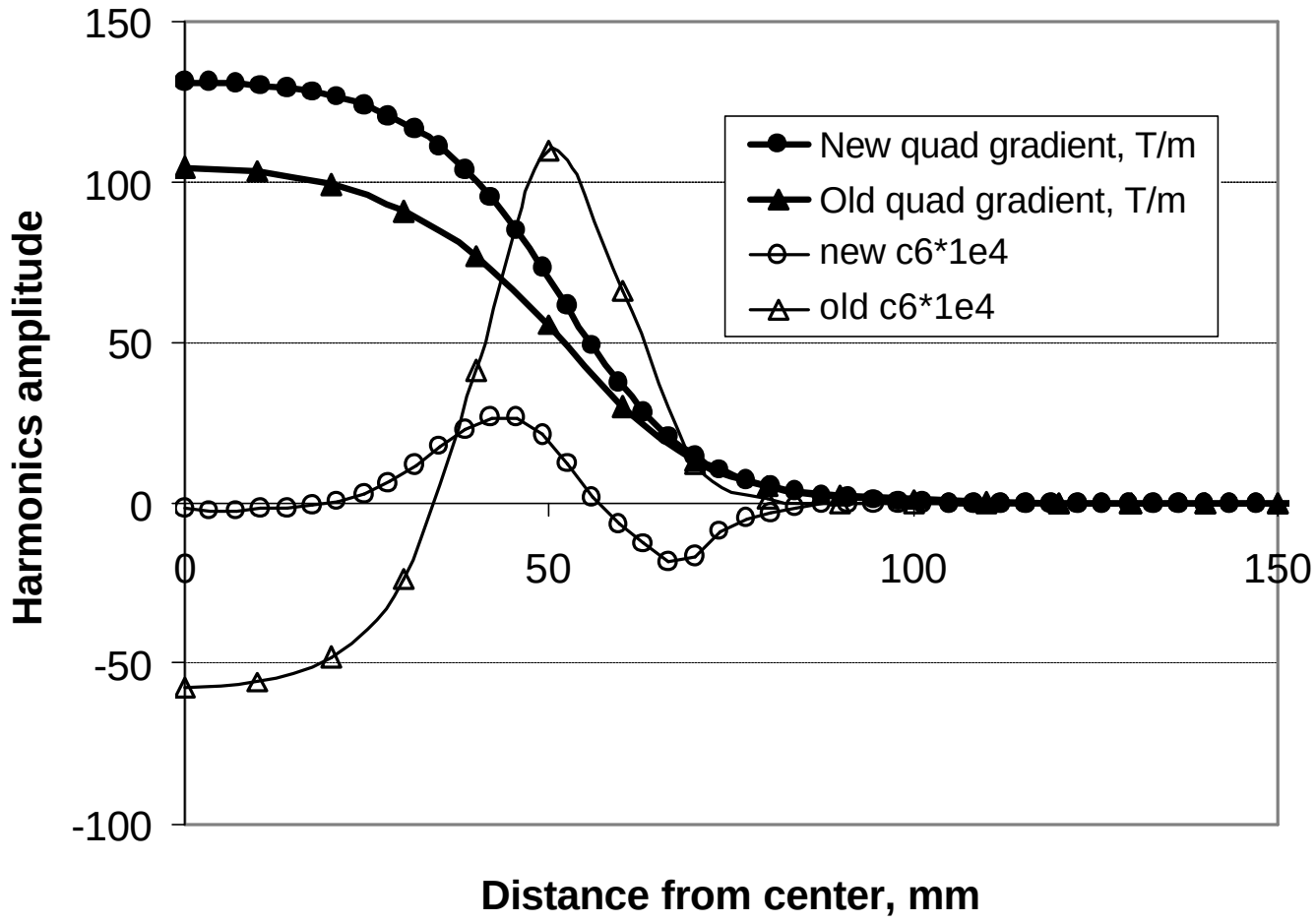
150
100
50
0
-50
-100
0
50
100
150
Harmonics amplitude
Distance from center, mm
New quad gradient, T/m
Old quad gradient, T/m
new c6*1e4
old c6*1e4

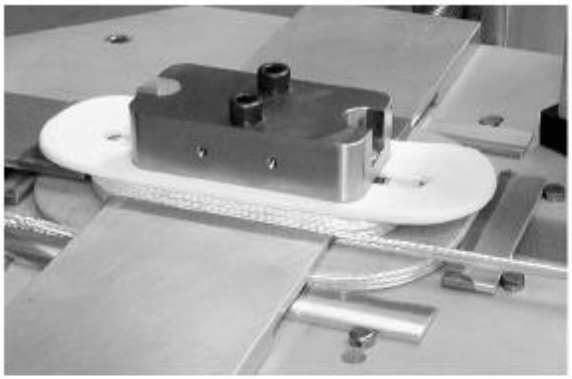


HCX

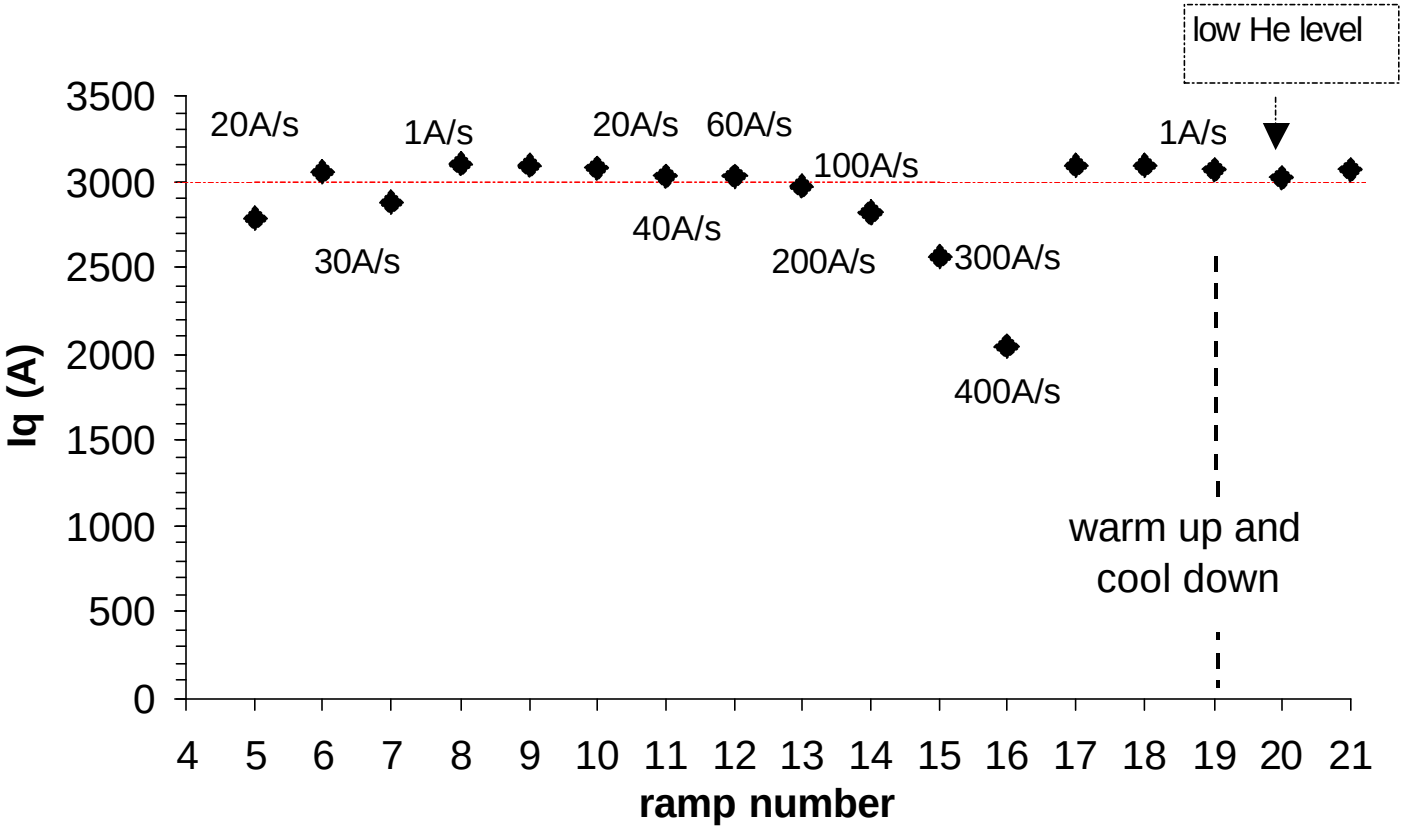
low He level
20A/s
30A/s
1A/s
20A/s
40A/s
60A/s
100A/s
200A/s
300A/s
400A/s
1A/s
warm up and
cool down
Iq (A)
ramp number
0
500
1000
1500
2000
2500
3000
3500
4
5
6
7
8
9
10
11
12
13
14
15
16
17
18
19
20
21

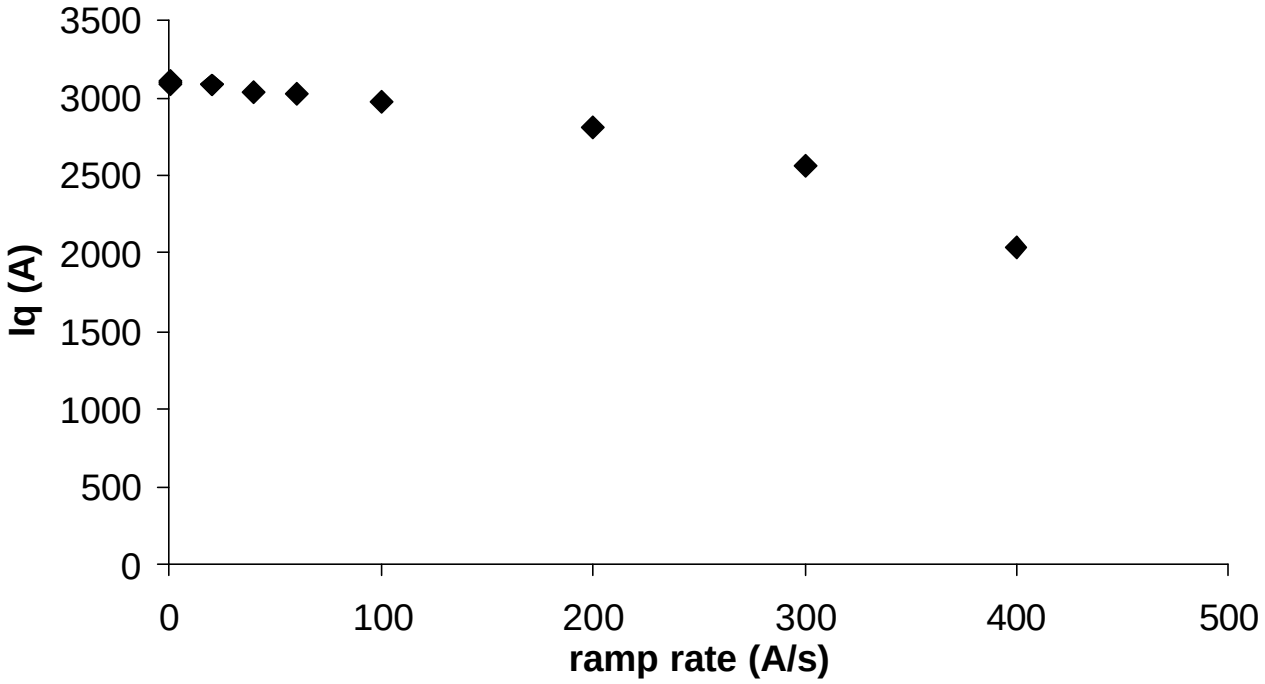
3500
3000
2500
2000
1500
1000
500
0
Iq (A)
0
100
200
300
400
500
ramp rate (A/s)

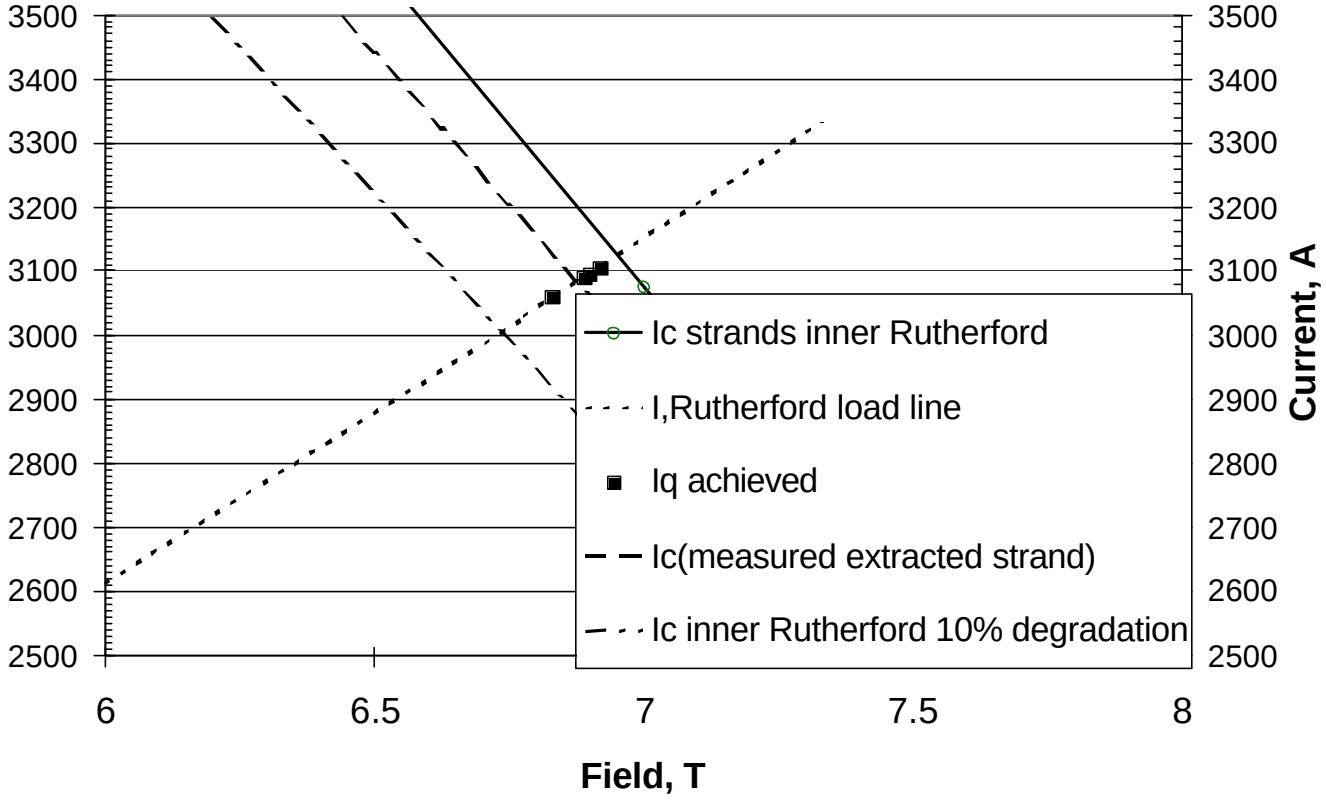
3500
3400
3300
3200
3100
3000
2900
2800
2700
2600
2500
6
6.5
7
7.5
8
Field, T
Current, A
Ic strands inner Rutherford
I,Rutherford load line
Iq achieved
Ic(measured extracted strand)
Ic inner Rutherford 10% degradation

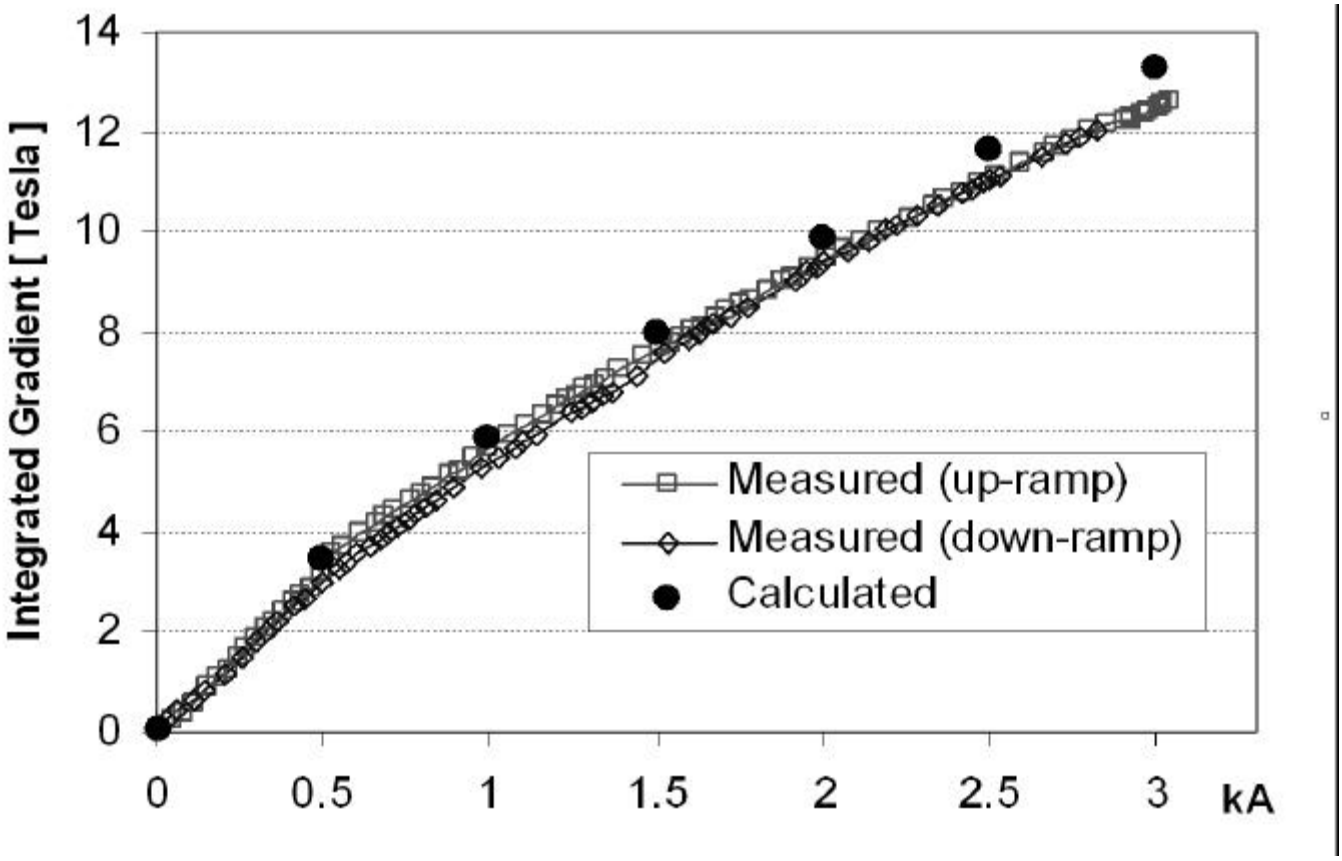
Integrated Gradient [Tesla]
14
12
10
8
6
4
2
0
0
0.5
1
1.5
2
2.5
3
kA
Measured (up-ramp)
Measured (down-ramp)
Calculated

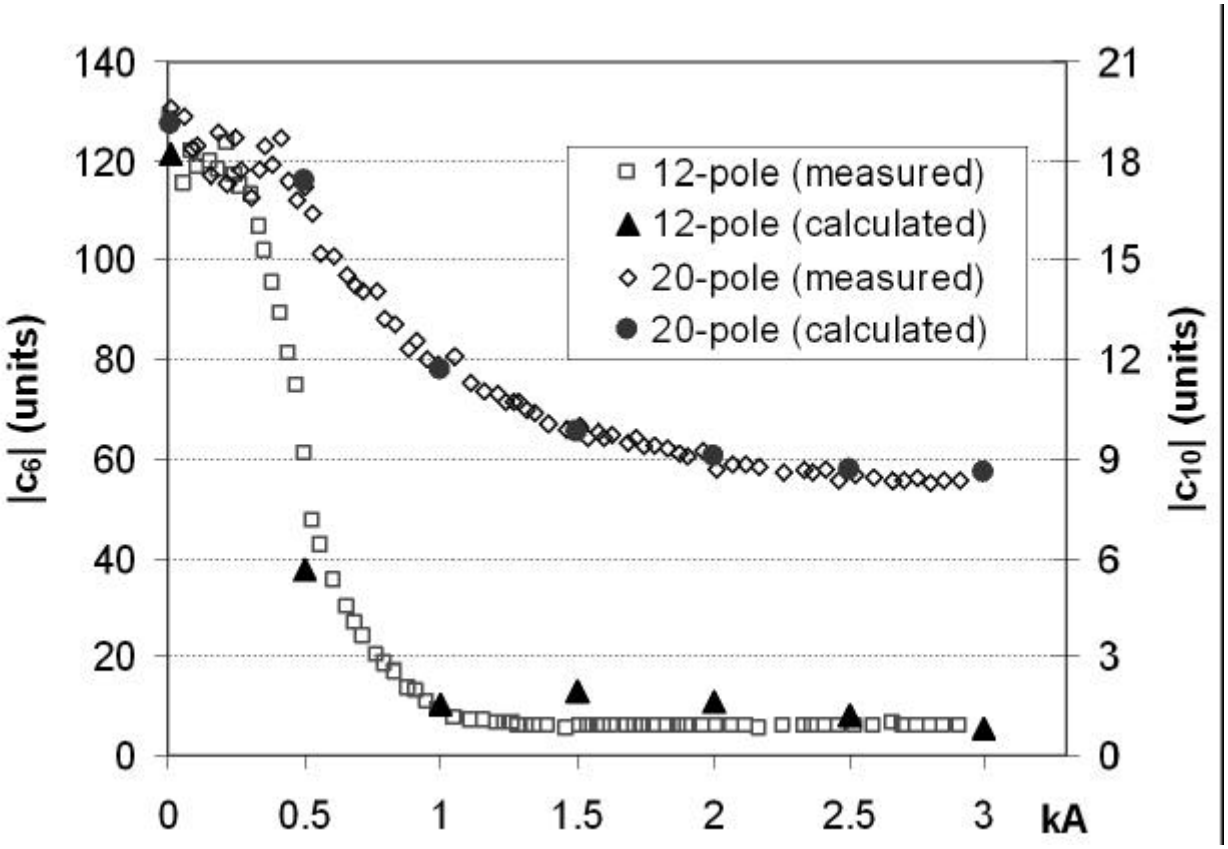
140
120
100
80
60
40
20
0
21
18
15
12
9
6
3
0
0
0.5
1
1.5
2
2.5
3
kA
|c6| (units)
|c10| (units)
12-pole (measured)
12-pole (calculated)
20-pole (measured)
20-pole (calculated)

TABLE I
INTEGRATED HARMONICS

Current (A)	Temp (K)	Data type	Gradient B_2/r_0 (T)	12-pole $\|c_6\|$ (units)	20-pole $\|c_{10}\|$ (units)
9.5	300	Meas. (*)	0.0674	109	15.5
9.5	-	Calc.	0.0726	121	19.1
2500	4.2	Meas.	11.03	5.8	8.5
2500	-	Calc.	11.63	8.1	8.7

(*) Averages for ± 9.5 A current and clock/counterclockwise probe rotation

TABLE II
NON-ALLOWED HARMONICS VS RANDOM ERRORS (1 SIGMA)

Order *n*	Measured $\|c_n\|$ (units)	Random- Block $\|c_n\|$ (units)	Random-Quadr. $\|c_n\|$ (units)
3	5.3	2.7	6.5
4	2.5	1.8	1.8
5	7.0	0.8	0.3
7	0.6	0.2	0.5
8	1.0	0.1	0.3
9	2.8	0.05	0.1